Formation of metastable excited Ti and Ni atoms during ion sputtering

G. Nicolussi, W. Husinsky, D. Gruber, and G. Betz
Institut für Allgemeine Physik, Technische Universität Wien, Wiedner Hauptstrasse 8-10, A-1040 Wien, Austria
(Received 27 June 1994; revised manuscript received 5 October 1994)

Metastable excited neutral Ti and Ni atoms in electronic states with energies up to approximately 0.2-eV excitation energy, ion sputtered from polycrystalline samples, have been analyzed with respect to their relative population and their velocity distribution. The influence of the electronic configuration (a^3F for Ti and a^3F and a^3D for Ni) on the population and energy distribution has been investigated. The targets have been bombarded with 8.0 keV Ar^+ ions under a 45° angle of incidence. The sputtered secondary neutrals were ionized by resonant one-color two-photon laser radiation and mass analyzed in a time-of-flight mass spectrometer. The population of all excited metastable states in the energy regime up to 0.1 eV have been found comparable to the ground-state population. The velocity distribution of the ground and excited states, regardless of their excitation energy and electronic configuration, have been found identical and governed by the collision cascade following the ion impact.

I. INTRODUCTION

The flux of secondary particles ion sputtered from metal surfaces consists of atoms, molecules, and clusters. These species can leave the surface in a variety of excited and charged states. From clean metals, the majority is emitted as neutral atoms in the electronic ground state. Despite the relative small contribution of non-neutral, non-ground-state particles, knowledge of the mechanisms responsible for charged and excited particle emission are important for the understanding of inelastic phenomena during the ion-solid interaction. However, a conclusive picture of the physics is not available.

In the collision cascade model for sputtering,[1] electronic processes can be taken into account only as a kinetic energy loss of the cascade atoms. A universal physical model of the mechanisms of the electronic excitation and deexcitation process is, however, not easily known. Several models and theories which try to describe a specific part of the entire excitation-deexcitation-emission process have been proposed in the literature.[2–4] A summary of the subject has been given by Yu.[5]

The essential difficulty arises when one tries to obtain information about the different possible excitation (ionization) and deexcitation (neutralization) processes from experimental results, because the data always show a convolution of all these possible processes. However, one can expect, as outlined later in this section, to obtain important clues for deconvoluting the different mechanisms from both the measurement of the abundance of excited atoms in the different electronic states and the energy distribution of the atoms emitted in theses states.

In the following a possible scenario leading to the emission of excited sputtered particles is outlined. Immediately after an atom escapes from the surface it can be either in a neutral ground state, a neutral excited state, or in an ionized state.[5] As far as the possible excitation processes are concerned, excitation of inner shell electrons can definitely occur in the cascade during the collision of atoms with high relative kinetic energy. As a consequence of these excitations, Auger electrons are emitted and have been observed experimentally.[6,7] Outer shell excitations of atoms during the final collision associated with the sputtering of a surface atom have also been discussed.[2] The population of valence electronic states during the collision cascade, however, poses a more severe problem. During the collision cascade the atoms involved represent a part of the solid; hence the existence of valence electronic states (in which the atom is later observed in the gas phase) has to be treated with some care. Nonetheless, recently the possibility of excitation of these states has been incorporated into a molecular-dynamics (MD) simulation treating the entire process chain for emission of sputtered excited atoms and yielding good agreement with specific experimental results.[8] Excited sputtered atoms can also be detected in the gas phase as a result of single knockon (recoils) by the incoming ion of a surface atom. Finally, collisions of emitted atoms above the surface can lead to excitations and has been identified in MD calculations.[8,9]

If we assume that the atom is in an excited state after the final collision resulting in sputtering, it can be nonradiatively deexcited due to the electronic interaction of an electron with the conduction band of the solid. This interaction is restricted to a few Å above the surface. The cross section for this deexcitation depends on the overlap of the wave function of the atom and the solid, hence on the specific electronic configuration of the excitation level observed. Furthermore, a significant dependence of the deexcitation probability on the velocity of the escaping atom should be assumed. In general, a dependence of the form $\exp(-A/a\,v_\perp)$ is expected, where a and A are ion-target specific parameters and $v_\perp$ is the emission velocity in the direction of the surface normal. This expresion was originally introduced by Hagstrum[10] to describe the neutralization probability of positive ions at the surface. It is

also well established that electronegative adsorbates (in particular oxygen) on the surface result in a substantial (sometimes up to two orders of magnitude) increase of the amount of sputtered excited atoms.[11] Several explanations of this effect have been proposed, ranging from a change in the work function of the oxidized surface to bond-breaking processes.[3–5]

The experimental method used in the experiments performed and described in the following sections is restricted to the investigation of atoms in excited metastable states. Since no fundamental difference in the physics of the formation and nonradiative deexcitation of atoms in metastable states and those in states with allowed electric dipole transitions to lower levels is obvious, we can assume that the results obtained can easily be extended to sputtered excited atoms in general. So far, most work concerning sputtered metastable atoms has been obtained with laser-induced-fluorescence[12–17] (LIF) and the study of emitted light by excited atoms. Recently new measurements of sputtered atoms in metastable excited states have been performed with resonant ionization spectroscopy (RIS).[8,18]

II. EXPERIMENTAL DETAILS

Polycrystalline titanium and nickel were bombarded under a 45° angle of incidence with Ar^+ ions of 8.0 keV energy and 1.5 μA current from a Colutron ion source; the primary ion flux density was around 10^{16} Ar^+ ions/s cm^2. The base pressure in the UHV chamber was approximately 5×10^{-9} mbar.

Since the yield of atoms sputtered in excited states might strongly depend on impurities, in particular, oxygen on the surface, it was necessary to clean the sample. This was achieved *in situ* by sputtering with a continuous ion beam, which was rastered across a surface area of about 2 mm × 2 mm for a few minutes before the measurement. Secondary neutral mass spectroscopy (SNMS) was used to check the surface composition with respect to impurities, in particular oxides. Within the sensitivity of SNMS, no measurable surface contaminants have been detected immediately after cleaning. Therefore, for measurements with a continuous primary ion beam, the influence of oxygen or other impurities can be assumed to be minimal. For measurements of the velocity distributions, where the ion beam has to be pulsed, regular dc sputter cleaning also ensured identical surface conditions. However, in order to keep ion-beam-induced surface damage minimal, the total dose of Ar^+ ions has to be kept low. The possible influence of the surface roughness on the velocity distribution will be discussed later. Ionization of secondary neutrals was achieved by radiation from a tuneable dye laser pumped by an excimer laser operating at 308 nm (XeCl). The sputtered secondary neutrals in different electronic states have been analyzed by one-color two-photon post-ionization in the wavelength regimes around 360 and 290 nm, respectively. For the measurements in the 290 nm range, the fundamental wavelength of the dye-laser output was frequency doubled. The distance d from the sample to the center of the focused laser beam was around 4 mm. The laser beam and target surface were parallel to each other; the dimension of the laser focus was approximately 0.2 mm in diameter.

Operating with wavelengths in the near-UV regime makes two-photon ionization possible for most metals. In order to identify a specific electronic state, the wavelength has to be tuned to an atomic resonance transition from this state to an intermediate state. Absorption of a second photon leads to ionization of the atom. Since the cross section of this resonant process is orders of magnitudes higher than for nonresonant two-photon ionization,[19] the photoions originate predominantly from one electronic state.

After post-ionization the particles were accelerated and mass analyzed in a time-of-flight (TOF) spectrometer. Measurements were performed in two different geometries of the TOF spectrometer. In the first operating mode, an ion mirror (reflectron) was used in the TOF path. This geometry yields high mass resolution and suppresses secondary ions created at the target surface. Since the transmission of the reflectron is not uniform for all particle velocities and, furthermore, acts as a low pass filter, the velocity measurements were performed in a straight TOF geometry without reflectron.

Analysis of the velocity spectra of sputtered atoms by a combination of laser post-ionization and time-of-flight techniques was recently performed by several groups.[8,20–22] The flight time of the secondary neutrals from the sample surface to the ionization volume ($d \approx 4$ mm) is determined by setting a delay t between the primary ion pulse and the laser pulse. Measuring the exact distance d allows one to determine the particle velocity v. In order to obtain a high time resolution, it was necessary to use very short ion pulses with a half width of less than 100 ns. This is much shorter than the characteristic drift times of the neutrals from the target to the ionization volume (typically between 200 and 5000 ns). Only particles emitted within a narrow angle around the surface normal were detected with the TOF spectrometer. Therefore, all secondary neutrals have nearly the same drift length d from the surface to the ionization volume. A more detailed description of these experimental details has been previously presented.[22]

III. RESULTS

At this point we would like to stress the following fact, which is important for the understanding of the experimental velocity (TOF) spectra presented in the following and also for the comparison of these data with experimental results obtained under different conditions and by other groups.

The experimental row data are flight time distributions. The SNMS signal is recorded as a function of the flight time of the particles between the sample surface and the laser beam. These data can easily be converted into velocity or energy distributions, taking into account the scale transformation of the ordinate.

Theoretical models, in general, yield an analytical ex-

pression for the particle flux (or particle density) distribution of the sputtered particles as a function of the kinetic energy. For the energy range and mass of primary ions used in this paper, it is well established that the *Thompson distribution*[23] describes the energy of sputtered neutral atoms in the electronic ground state quite well.[24] Therefore, it is useful to compare the experimental energy distributions of sputtered particles with the Thompson distribution, which means comparing unknown distributions with the distribution of sputtered neutral ground-state atoms. The Thompson formula gives the particle flux distribution $f(E)$ in the form

$$f(E) \propto E/(U_b + E)^{n+1} , \quad (1)$$

where E is the kinetic energy, U_b is the surface binding energy, and n represents a fit parameter. The Thompson formula is also often presented as a particle density distribution $n(E)$. Since $f(E) = n(E)\,v$ and $v \propto \sqrt{E}$, the density distribution can be expressed in the form $n(E) \propto \sqrt{E}/(U_b + E)^{n+1}$.

An important question is whether the measured SNMS signal is proportional to the *particle flux through the ionization volume* or to the *particle density in the ionization volume.* In the most general case, the detected SNMS signal will consist of a density *and* a flux contribution.[21] For our pulsed laser system the expected signal is, in a first approximation, proportional to the particle density. However, for certain experimental parameters, e.g., high particle velocities and high ionization cross sections, the signal can deviate from the density distribution towards a flux distribution.

In order to compare the measured distributions with the Thompson distribution, we have, therefore, incorporated the experimental conditions (dimension of the ionization volume, length of laser and ion pulse, ionization efficiency, etc.) via a computer modeling of the experiment. The measured signal was simulated by combining the particle emission process (Monte Carlo–type random particle emission assuming a Thompson velocity distribution) and the post-ionization of the particles with the specific geometry and SNMS parameters. By varying the parameters of the Thompson distribution and comparing the measured and simulated spectrum we can thus directly check the validity of the Thompson distribution for the energy (velocity) distribution in question.

A. Titanium

Ti atoms have been sputtered from a polycrystalline Ti target. For Ti, the three levels of the electronic ground-state triplet are accessible for investigations. The energies of the excited levels in the ground-state configuration $a\,^3F$ are relatively small (0.02 and 0.05 eV). The electronic configuration of the multiplet is characterized by two s electrons, which should act as a good shield for possible interactions of the d electrons when leaving the surface. Therefore, the cross sections for deexcitations in the surface region are, according to the general belief, expected to be small or negligible. Furthermore, metastable excited states exist with excitation energies around 0.9 and 1.4 eV. These excitation energies are relatively high for sputtered atoms. With one exception,[18] no experimental results performed with post-ionization methods exist for sputtered atoms in very high excited metastable states (several eV excitation energy).

We have attempted to identify atoms in the metastable excited states with energies above 0.9 eV, but did not succeed in obtaining a signal. The reasons for that will be discussed later together with the results for Ni. The experiments for Ti described in the following, therefore, are restricted to the metastable states of the ground-state multiplet.

We have used two different wavelength regimes for the resonant excitation (ionization) of specific electronic states of sputtered atoms. Basically, identical results have been obtained for both sets of experiments. In the following the discussion will be restricted to results obtained with resonant excitations in the wavelength regime around 290 nm (frequency-doubled Rhodamin 6G). Using the regime above 360 nm some complications and interesting features arise for the ionization process due to two-photon absorption of Ti ground-state atoms into Rydberg states. This highly excited atoms can ionize easily due to the extraction field ($\approx$ 5000 V/cm) of the mass spectrometer. This results in "resonant" features in the ionization spectrum due to Rydberg states or autoionizing levels. More details concerning these results will be published elsewhere.

The Ti photoion signal as a function of the wavelength of the resonant excitation is shown in Fig. 1. Resonances are observed which correspond to resonant transitions from the ground-state triplet $a\,^3F$ to the intermediate level $v\,^3F^0$. The corresponding J values, transition wavelengths, energy levels, and transition probabilities are summarized in Table I.[25]

The intensity of the laser radiation was approximately 10^7 W/cm^2. Saturation of the ionization could not be achieved in most cases. On the one hand, this can be concluded from the fact that the signals from an identical initial state via different intermediate states vary in intensity. On the other hand, it has been verified by changing the laser intensity. The transitions probabilities of the lines shown in Fig. 1 vary approximately within one order of magnitude. Since saturation of the first resonant excitation step $a\,^3F$-$v\,^3F^0$ should be achieved easily with the laser intensities used, the cross section of absorption of the second photon seems to determine the efficiency of the ionization and thus the measured photoion signal.

TABLE I. Transitions from the Ti I ground state $a\,^3F$ to $v\,^3F^0$.

J_i-J_k	λ [nm]	E_i [cm^{-1}]	E_k [cm^{-1}]	A_{ki} [10^8 s^{-1}]
4-4	295.61	386.9	34 205	0.97
3-3	294.83	170.1	34 079	0.93
2-2	294.20	0.000	33 981	1.00
4-3	296.72	386.9	34 079	0.11
3-2	295.68	170.1	33 981	0.18
3-4	293.73	170.1	34 205	0.077
2-3	293.35	0.000	34 079	0.096

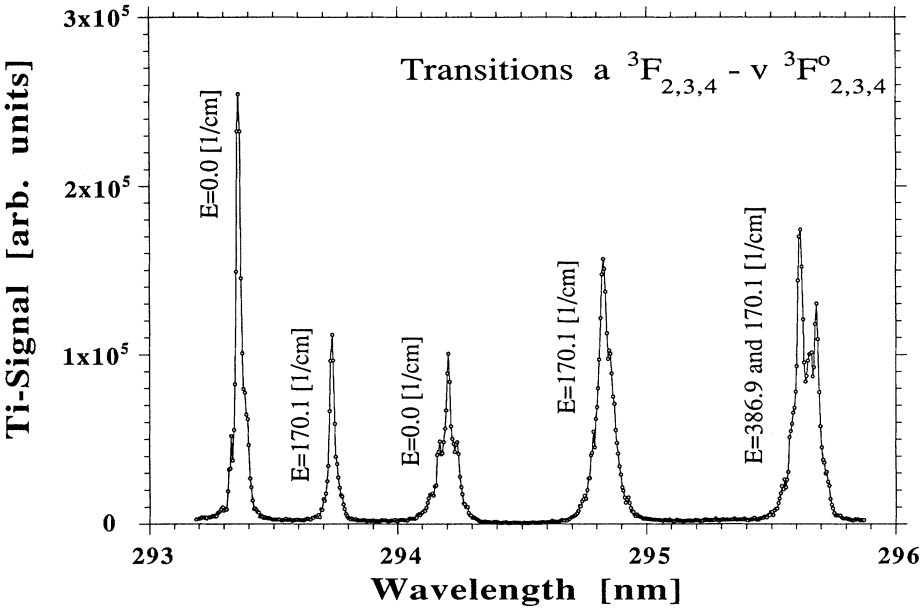

FIG. 1. Ti photoion signal as a function of the post-ionizing laser wavelength (λ = 293–296 nm): The RIS peaks correspond to resonant transitions from the ground-state triplet a^3F to the intermediate level v^3F^0. The intensity of the laser radiation was approximately 10^7 W/cm^2. The nonresonant two-photon ionization of Ti neutrals is negligible for this wavelength range and the laser intensities used.

During the scan shown in Fig. 1 the laser intensity, due to the efficiency change of the laser dye and the frequency doubler crystal, might roughly vary by a factor of 2.

As a consequence of the facts outlined above, an exact and reliable quantitative determination of the population of the metastable levels of the ground-state multiplet is always left with an error bar of an order of magnitude. We can, however, conclude from the measurements and the known oscillator strengths of the Ti lines involved that all levels (including the ground state) are populated after the sputtering process within the same order of magnitude.

In order to determine the accuracy of the velocity spectra, the following facts have to be considered. The flight time of the particles has an absolute error of approximately ± 20 ns, since the zero point of the time scale cannot be determined with higher accuracy. As a consequence, for short flight times (below $\approx$ 200 ns) the relative error can be high and, hence, the velocity distribution for kinetic energies above 100 eV exhibits an increasing substantial error bar on the energy axis. On the other hand, the interesting energy range of the spectra presented in the following lies between 0 and 100 eV, where the accuracy of the measured energies is very good. The error of the SNMS signal is basically of statistical nature. By increasing the number of summed spectra (1000 per data point in this measurement) the statistics can be improved; on the other hand, keeping well-defined surface conditions over a long time period is difficult.

The measured TOF distribution of atoms sputtered in the states of the ground-state configuration a^3F states is shown in Fig. 2. The main result which can be obtained from Fig. 2 is that the distributions are, within the experimental error, identical for particles sputtered in any of these levels. The TOF spectra in Fig. 2 are in good agreement with the theoretical Thompson distribution $n(E) \propto \sqrt{E}/(U_b + E)^{n+1}$, describing the particle density. The best fit of the spectra was achieved with n equal to 2 and for a surface binding energy U_b of 4.85 eV in agreement with the tabulated heat of sublimation of Ti. Under good agreement we understand that the Monte Carlo-simulated distribution is within the statistical error of the measurement identical with the measured distribution. In particular, the maximum and high-energy falloff of the distribution must be reproduced by the simulation. These results are also in agreement with LIF measurements reported previously.[15] Measurements of the velocity distribution, which we performed using laser radiation in the wavelength regime around 360 nm, yielded identical results. This is quite important, as it proves that the velocity distribution is not influenced by the excitation (ionization) process. Information about the population of the individual states, however, is much more reliable for the 290 nm regime because correlation between a measured resonant signal and a specific excited state of the sputtered atom can be much more easily achieved.

B. Nickel

Investigations of sputtered excited Ni atoms offer an interesting additional feature. Beside the ground-state multiplet a^3F, a second electronic multiplet a^3D exists with the following characteristics: (a) The lowest multiplet state lies 0.025 eV above the Ni ground state and (b) it has a different electronic configuration than the ground state. The atomic energy levels[25,26] of these two multiplet configurations of Ni, both being triplets, are listed in Table II. The excited a^3D triplet is characterized by *one* outer s electron, the ground-state configuration a^3F by *two* outer s electrons. Following the arguments of Winograd, a different behavior with respect to deexcitation processes of the Ni atoms at the surface can be expected from the different valence electron configurations.[8]

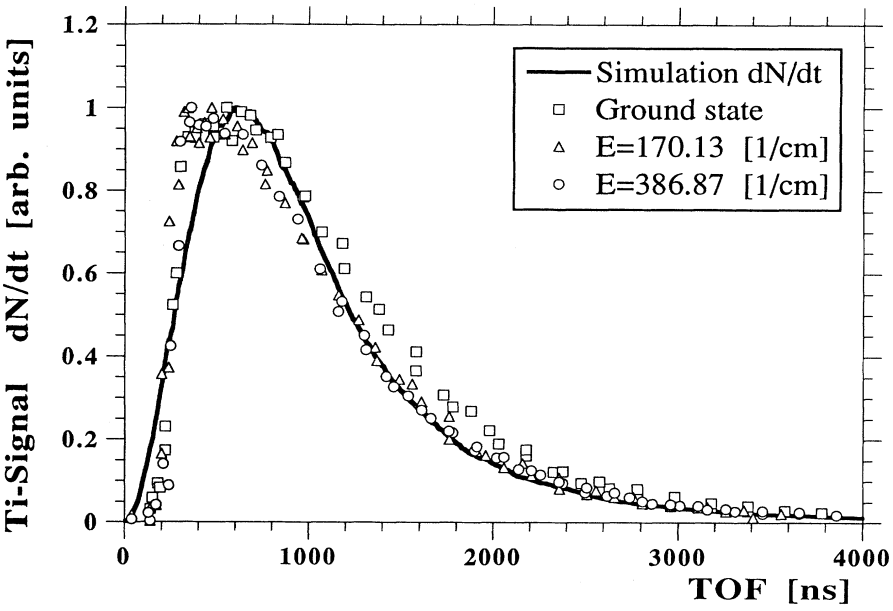

FIG. 2. TOF distribution of Ti atoms sputtered in the ground-state configuration a^3F: The distributions are, within the experimental error, identical for Ti atoms sputtered in any of the sublevels of the multiplet. The TOF spectra are in good agreement with the theoretical Thompson density distribution $n(E) \propto \sqrt{E}/(U_b + E)^{n+1}$. The best fit of the spectra was obtained with $n = 2$ and for a surface binding energy $U_b = 4.85$ eV in agreement with the tabulated heat of sublimation of Ti.

The photoion signal of nickel was investigated in the same wavelength range and under the same experimental conditions as for the Ti measurements. Two wavelength scans for Ni are shown in Figs. 3 and 4. Similar to the situation for Ti, saturation of the photoion signal was not achieved, with the one exception for the transition a^3D_3 ($E_i = 204.8$ cm^{-1}) to $y^3D_3^0$ at $\lambda = 300.248$ nm. In this case nearly 100% ionization efficiency could be observed. As a consequence, the same conclusions as for the Ti measurements have to be drawn with respect to quantification of the population of the different sublevels of the two multiplets. It should be pointed out that in spite of the saturated ionization for the laser wavelength $\lambda = 300.248$ nm, the observed extremely high photoion signal could be a consequence of a relatively high population of atoms sputtered in the excited a^3D_3 state.

In contrast to the titanium resonant photoion signal, a very high nonresonant background was observed in the entire wavelength range investigated. This nonresonant signal amounts to approximately 2% of the maximal resonant signal at $\lambda = 300.248$ nm. From previous investigations,[22,27] we have strong evidence that this nonresonant atom signal is caused predominantly by positively charged atoms, which originate from laser-induced dissociation of clusters. The origin of the signal due to clusters is easily determined from the velocity distribution, which is shifted to lower cluster velocities.[22] The energy distribution of clusters, A_N (consisting of N atoms A), peaks approximately at the same energy as the distribution for atoms, A, but the velocity distribution peaks (in accordance with the higher mass) at lower velocities. If, e.g., Ni_2 dimers dissociate in the laser beam into positive charged atoms Ni^+, the signal in the atom channel is enhanced by these fragments, but the velocity distribution of these artifacts still exhibits the dimer velocity distribution. Since the cluster yield of nickel, in particular the dimer yield, is much higher than the one for titanium, the effect is much more pronounced in this case.[28,29] Furthermore, dissociation of Ni dimers can be achieved by single-photon absorption in the wavelength range around 290 nm.

TABLE II. Ground-state configuration and first excited configuration of Ni I.

Configuration	Term	J	Level [cm^{-1}]
$3d^8\,4s^2$	a^3F	4	0.000
		3	1332.15
		2	2216.52
$3d^9(^2D)\,4s$	a^3D	3	204.79
		2	879.813
		1	1713.08

In Fig. 5 the $1/v$ distribution of sputtered Ni atoms in the excited a^3D_3 is shown. Comparison with the theory (the procedure including the experimental parameters described earlier in this paper has been used) again demonstrates the excellent agreement with a Thompson distribution ($n = 2$ and $U_b = 4.44$ eV). The RIS signal of the level a^3D_3 at $\lambda = 300.248$ nm is somehow an exception among the other states shown in Fig. 3, because the nonresonant contribution amounts to only 2% of the resonant signal in this case. As a consequence, the velocity distribution can be regarded as representative for the atoms in this state.

As far as the velocity distribution of atoms in the ground-state and other multiplet levels are concerned, the signal at the respective resonant wavelength consists of a resonant (characteristic for the specific state) and a substantial nonresonant contribution. As we have shown previously, the nonresonant signal itself arises from nonresonant ionization of Ni atoms in the various states and from fragmentation of clusters. Therefore, the velocity distributions have to be treated with caution if the nonresonant contribution is high. Indeed, we observe (see Fig. 6) a shift and broadening of the velocity distri-

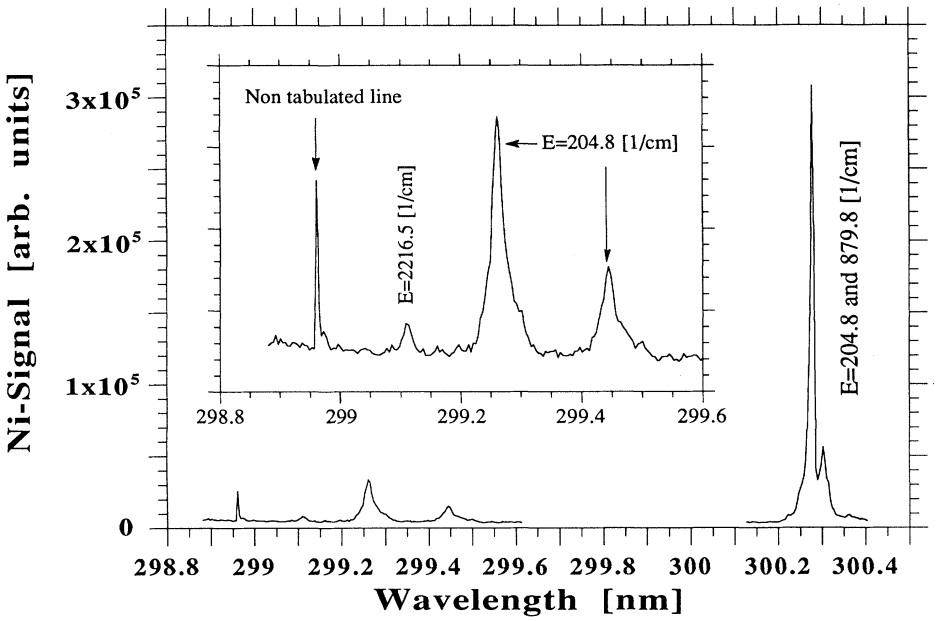

FIG. 3. Ni photoion signal as a function of the post-ionizing laser wavelength (λ = 298.8–300.4 nm): Saturation of the photoion signal was only achieved for the transition a^3D_3 (E_i = 204.8 cm^{-1}) to $y^3D_3^0$ at λ = 300.248 nm. Generally, we find stronger signals for the a^3D_3 state than for the ground-state a^3F_4, regardless of the intermediate resonance level.

butions (to lower velocities) in all cases, where a substantial nonresonant contribution is observed. In Fig. 6 the distribution for atoms in the a^3D_2 state (the same is also valid for atoms in the ground state a^3F_4) is shown. In addition, the velocity distribution obtained with purely nonresonant ionization at an off-resonance wavelength of 298 nm is shown in Fig. 6. This nonresonant distribution is also observed at any off-resonance wavelength in Figs. 3 and 4. The trend in the velocity distributions caused by the nonresonant contribution is evident and can be understood by the influence of clusters. The nonresonant Ni atom distribution in Fig. 6 would rather agree with the

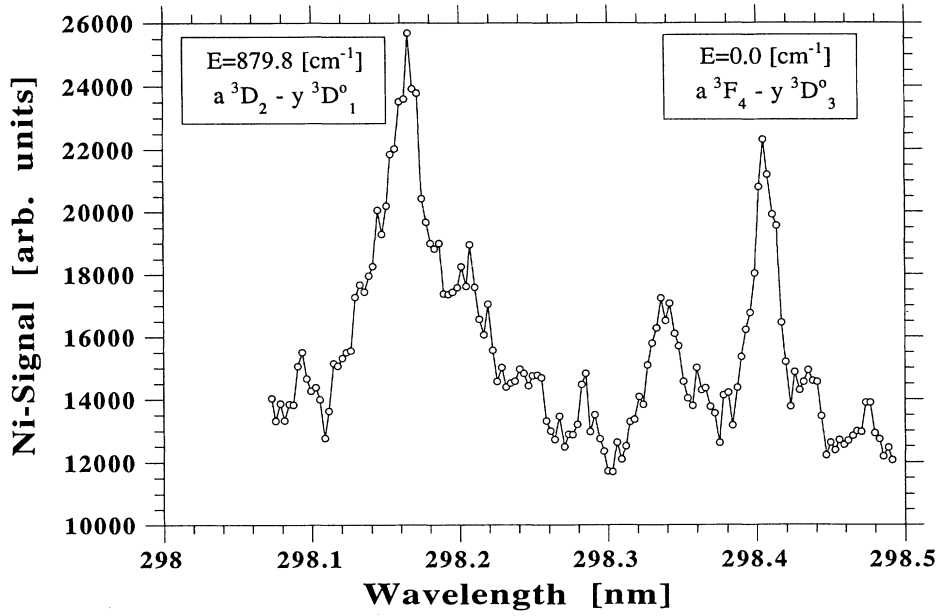

FIG. 4. Ni photoion signal as a function of the post-ionizing laser wavelength (λ = 298.0–298.5 nm): In contrast to the titanium measurements, a very high nonresonant background was observed in the entire wavelength range investigated. At a wavelength of 298.16 nm the resonant contribution from the transition a^3D_2-$y^3D_1^0$ amounts to only about 50% of the total signal. For the other resonant transitions a^3F_4-$y^3D_3^0$ (298.41 nm) or a^3F_2-$y^1F_3^0$ (299.11 nm) the "signal-to-noise" ratio is even worse. The problem cannot be improved by increasing the laser power, since the saturation of the resonant contribution would be accompanied by an enhanced nonresonant signal.

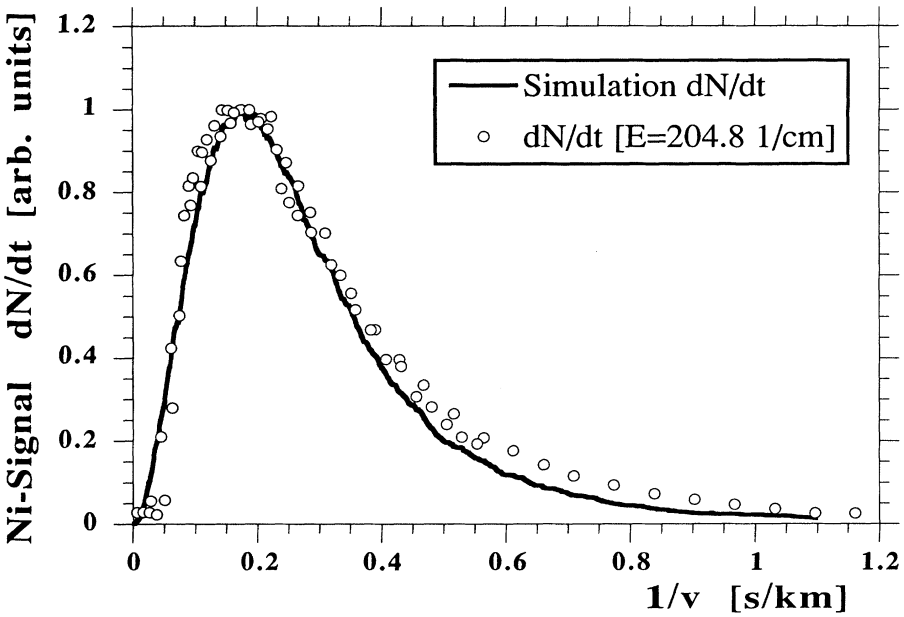

FIG. 5. $1/v$ distribution of sputtered Ni atoms in the excited state $a\,^3D_3$: The $1/v$ distribution of Ni atoms in the electronic state $a\,^3D_3$ (E_i=204.8 cm^{-1}) was determined by resonant ionization of Ni atoms via the intermediate state $y\,^3D_3^0$ with the transition wavelength λ = 300.248 nm. Excellent agreement with a Thompson distribution expected for ground-state atoms was observed (fit parameters $n = 2$ and $U_b = 4.44$ eV).

expected Ni_2 distribution. In the last two years, measurements of energy distributions of sputtered metal clusters by nonresonant laser post-ionization[20–22,27,30] have been attempted successfully. These investigations have also shown that experimental results can be affected by the influence of cluster dissociation.

In principle we have observed all allowed transitions from the two terms $a\,^3F$ and $a\,^3D$ in the considered wavelength range, but most of the RIS peaks are weak. The situation is best seen in Fig. 4, for a resonant wavelength of 298.16 nm the resonant contribution from the transition $a\,^3D_2$-$y\,^3D_1^0$ is about 50% of the total photoion

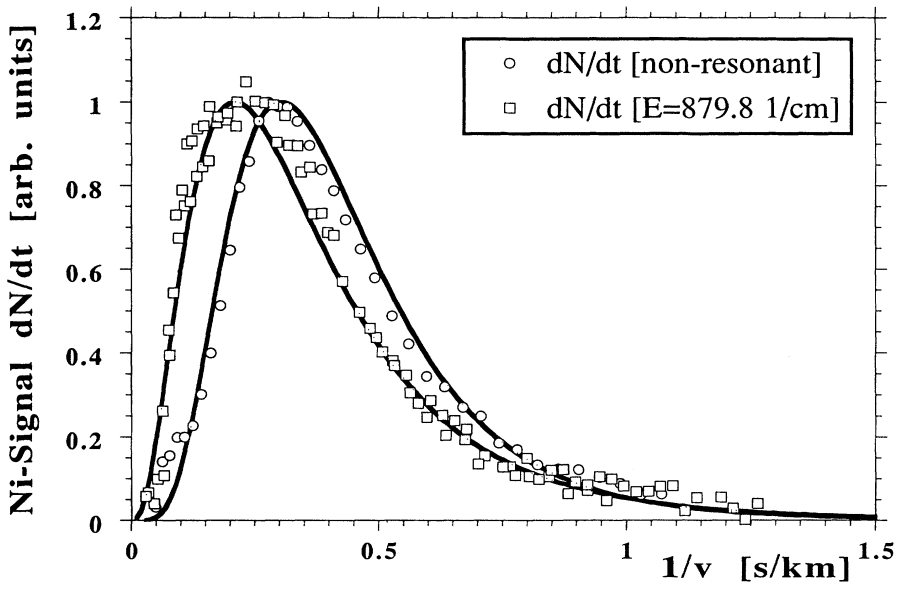

FIG. 6. $1/v$ distribution of sputtered Ni atoms in the excited state $a\,^3D_2$ and TOF ($1/v$) distribution of Ni atoms from nonresonant laser radiation: The $1/v$ distribution for atoms in the $a\,^3D_2$ (E_i = 879.8 cm^{-1}) was determined by resonant ionization via the intermediate state $y\,^3D_1^0$ with the wavelength λ = 298.16 nm. In addition, the velocity distribution obtained by purely nonresonant ionization at an off-resonance wavelength of 298 nm is shown. The dashed and the solid lines are best fits through the data points to guide the eye. The trend in the velocity distributions caused by the nonresonant contribution is evident and can be understood by the influence of clusters.

signal. For the other resonant transitions $a\,^3F_4$-$y\,^3D_3^0$ (298.41 nm) or $a\,^3F_2$-$y\,^1F_3^0$ (299.11 nm) the "signal-to-noise" ratio is even worse. The situation should not improve by increasing the laser power, because the saturation of the resonant contribution would also be accompanied by an enhanced nonresonant signal.

Detection of atoms sputtered in higher metastable excited states (in the eV range) is a difficult task, since they are generally very weakly populated. The nonresonant contribution to the photoion signal makes such an analysis almost impossible. The population of these states is expected to be lower by several orders of magnitude as compared to the ground state or very low excited states.[16,17,31,32] Since the nonresonant contribution arises from all populated states, even a very low nonresonant cross section will cause the resonant signal of these high excited states to be buried in noise.

However, one approach seems promising to avoid these inherent problems. We have tried to detect and identify high excited states by choosing a wavelength ($\lambda \approx 580$ nm, intensity 10^9 W/cm^2) which makes ionization of atoms in states below approximately 3.3 eV by two or one photon impossible. Only atoms in higher-lying levels could be ionized by two photons. However, there still remains the problem of cluster dissociation, especially the Ni dimer. Morse[33] reports a predissociation limit for Ni_2 of $16\,680 \pm 10$ cm^{-1} which corresponds to $D_0 = 2.068 \pm 0.01$ eV. If we tune the laser to the corresponding wavelength of 599.5 nm, we have, indeed, observed an enhanced Ni photoion signal, which can be attributed to dissociation of Ni_2.

On the other hand, for a wavelength of 580 nm we do observe only a very weak signal. It is well established that a strong increase of the yield of sputtered atoms in excited metastable states[12,17] is observed for sputtering from oxidized metal surfaces. This is true, even though the total atom sputter yield is decreased by the presence of oxygen on the surface.[12] For an oxygen partial pressure of about 5×10^{-7} mbar, the photoion signal using 580 nm laser radiation increased significantly, indicating that the signal, indeed, originates from atoms in highly excited states above 3.3 eV, which can be ionized with two 580 nm photons.

The relative magnitude of this signal to the saturated $a\,^3D_3$ signal at $\lambda = 300.248$ nm is approximately 10^{-3}. However, a second origin for this Ni signal is laser-induced fragmentation of NiO into Ni^+. Since the dissociation energy for NiO is $D_0 = 3.96$ eV, a nonresonant two-photon absorption is required.[34] Due to its low probability, this process should play only a minor role.

IV. DISCUSSION AND CONCLUSION

A general statement concerning experiments with atoms in excited states, in particular in low-energetic metastable ones, during sputtering is necessary at this point. The population of these low-lying metastable states is evidently influenced by cascading from higher-lying states with allowed dipole transitions to these metastable levels. The energetically lowest-lying levels which can feed the ground-state configuration of Ti are above 2 eV excitation energy and above 3 eV for the metastable Ni states investigated. In general, it is assumed that the overall population of sputtered atoms with electronic excitations in the eV range is far below the percent range. Under this assumption the influence of cascading to the measured data obtained in this paper should be rather minimal. However, recently a relative high population of a specific excited state during sputtering of Ag has been reported.[18] If similar populations of high excited states should prove to be of a general nature, cascading might severely influence measurements similar to the ones presented here.

The possible influence of the ion-beam-induced surface damage on the results is not fully clear at this stage. A very rough surface would lead to undefined impact and emission angles. As a consequence, the deexcitation processes between the sputtered atom and the surface may be affected. Remaining uncertainties could be cleared by future experiments comparing (at otherwise identical parameters) results for single-crystal and polycrystalline targets. On the other hand, many of the results published so far have been performed on polycrystalline targets and thus suffer from the same problem.

Information about the primary excitation mechanism should appear in the population of the different states. Previous measurements of the population of excited states have shown a decreasing abundance with the excitation energy of the level. In some cases measured relative populations as a function of the excitation energy[16,17,31,32] could be fitted with Boltzmann-like distributions and a characteristic fit "temperature." Moreover, it was found that for Fe this exponential behavior is only valid within *one* electronic configuration and different fit temperatures have been found for different configurations.[32]

In the RIS measurements presented here, the signal of atoms in a specific electronic state is proportional to the population of this state, but also proportional to the ionization efficiency. If the resonant ionization is saturated for different initial states, the relative signals should be equal to the relative population of these initial states. Unfortunately, the exact value of the ionization efficiency is unknown. From the laser power dependence of the RIS peaks we can roughly make an estimate of the "saturation signal." As a consequence of the facts outlined above (e.g., different transition probabilities of resonant excitations, variation of laser power due to laser dye, and frequency doubler efficiency) the ionization efficiency varies approximately within one order of magnitude. Taking into account the known oscillator strengths of the transitions, we can conclude from the measurements that all investigated levels for Ti and Ni with excitation energies below 0.1 eV are populated after the sputtering process within the same order of magnitude.

One interesting feature is that for Ni the highest RIS signal was observed (at the resonance wavelength of $\lambda = 300.248$ nm) for atoms sputtered in the state $a\,^3D_3$ with an excitation energy $E_i = 204.8$ cm^{-1}. Generally, we find stronger signals for the $a\,^3D_3$ state than for the ground state $a\,^3F_4$, regardless of the intermedi-

ate resonance level used. Even though the RIS signal for the transition wavelength $\lambda = 300.248$ nm was the only one in the Ni multiplet for which saturation of the post-ionization could be achieved, we cannot exclude the possibility that the Ni ground-state $a\,^3F_4$, from which the used resonant transition $a\,^3F_4$-$y\,^3D_3^0$ has a much lower (by a factor 50) oscillator strength, is less populated than the metastable state $a\,^3D_3$.

If one compares the data presented here with other measurements, it should be taken into account that the population of excited levels will depend on the primary ion energy, the angle of incidence, and the ion species. Only a few investigations have been done with respect to the dependence on ion energy. If we assume that gas phase collisions of atoms at a short distance above the surface are an important excitation mechanism, this process should depend strongly on the sputter yield and, as a consequence, on the primary ion energy. In some cases the sputter yield for excited atoms was found to be proportional to the total atom sputter yield as a function of the primary ion energy. Therefore, the relative population with respect to the ground state remains almost unchanged. Andersen *et al.*[35] have found this behavior for Au, Cu, and Zn; in contrast, for Ga atoms irregularities have been observed. The dependence of the yield of excited atoms on the angle of incidence can be quite strong for very oblique incidence, as has been observed for Al, Cu, and Ni.[36–38] Finally, the primary ion dose can play a role, because the sputter-induced surface roughness for high total doses leads to undefined impact and emission angles.

One of the basic questions in sputtering of excited states is the importance of the electronic configuration concerning the excitation and deexcitation processes. Is it possible to draw conclusions with general validity from the behavior of the Ti and Ni atoms sputtered in different electronic configurations? It has been argued that the relaxation times of collisional excited atoms depend rather on the electronic configuration than on the excitation energy. The concept of excitations (of valence-electronic states) during the collision cascade has to be regarded with some care, as outlined in the Introduction. Therefore, a physical description is problematic. Winograd and co-workers characterized a collisional excitation in his MD simulations by a critical distance $r_{\rm th}$ between two atoms in the collision cascade.[8,9] Whenever the approach of two atoms during a collision is closer than this threshold radius $r_{\rm th}$, the specific state is assumed to be excited. In addition, a relaxation time of the excited state has to be introduced for describing the entire process.

However, simulations of the excitation-deexcitation processes in the cascade poses a challenge. Finding proper criteria for a specific excitation mechanism (with defined excitation energies) is a difficult and debatable task. If we consider collisional excitation in the cascade, various electronic states can be involved in the excitation and deexcitation processes. The MD simulations performed so far deal only with two possible states, with the ground state and *one* excited state. This restriction to only two possible states is a strong simplification.

It should also be mentioned in this context that experimental measurements as well as MD simulations have shown that for impact energies in the keV range the majority of the sputtered flux originates from the first and second atomic layers.[39] Therefore, only the very last collision in the cascade sequence seems to be relevant for the electronic state of an atom immediately before leaving the surface.

However, we would like to point out that the experimental finding does not necessarily mean that excitations have to originate from the collision cascade. Other excitation mechanisms can lead to similar population distributions. Gas phase collisions of emitted particles above the surface[8] can be treated in analogy to collisions in the cascade, but with different survival times. The bond-breaking model[4] could also explain the existence of excited sputtered atoms and could explain the measured population distributions.[11] However, the bond-breaking mechanism is not reasonable for clean (oxygen-free?) metals and should gain importance for increasingly oxidized surfaces. The behavior under oxygen exposure for the low-lying Ti and Ni metastable states investigated rather implies a mechanism different from the bond-breaking case. On the other hand, preliminary measurements of higher excited metastable Ni states could be explained by this mechanism.

What can we now learn from the Ti and Ni measurements with respect to the deexcitation mechanism of excited atoms at the surface? A general conclusion can be drawn from the measured TOF $(1/v)$ distributions (Figs. 2, 5, 6) of atoms sputtered from polycrystalline Ti and Ni targets in excited metastable states with energies E_i below approximately 0.1 eV: The TOF $(1/v)$ distribution in all cases is identical to the distribution of atoms leaving the surface in the electronic ground state, which itself follows the theoretical Thompson distribution. The essential fit parameter of this distribution coincides with the heat of sublimation of the metal and the distribution shows a characteristic E^{-2} falloff for high emission energies.

Similar results have been obtained from LIF measurements of the velocity distribution of sputtered atoms in low-lying metastable states of Zr atoms belonging to the ground-state multiplet.[15] LIF measurements of the velocity distribution of atoms sputtered in higher excited states showed a shift to higher velocities and broadening of the distribution.[12,13] On the other hand, recent measurements using laser post-ionization[8,9] imply shifts in the velocity distribution for atoms sputtered in low-lying metastable states belonging to the ground-state multiplet. This contradiction to our measurements cannot be explained adequately at this moment.

Hence, from our measurements no influence of the electronic configuration (angular momentum) or the excitation energy can be derived in the range of low excitation energies (< 0.1 eV). This implies that either for particles in low-energetic excitation states deexcitation processes at the surface are of no relevance or that the excitation happens after the surface-atom interaction due to overlap of the wave functions.

The situation for highly excited states might be different. We have mentioned above that the analysis of

high excited (and weakly populated) secondary neutrals with one-color two-photon post-ionization can be complicated by the influence of nonresonant ionization[19] of higher populated states. Also contributions from laser-induced cluster dissociation can play a role for the atom signal.[27] As a consequence, resonant signals much weaker than the nonresonant background cannot be identified. To avoid these difficulties measurements of highly excited metastable states should be performed with less energetic wavelengths, which do not produce significant nonresonant contributions. This can be achieved for example by operating in wavelength regimes where two-photon ionization from the ground-state multiplet is not possible; presently such experiments are in preparation. Preliminary results indicate differences in the behavior of the population, in particular with respect to surface oxidation, of excited sputtered particles.

ACKNOWLEDGMENTS

We would like to acknowledge the financial support by the Österreichische Fonds zur Förderung der wissenschaftlichen Forschung under Project No. P8706-PHY. We would also like to thank N. Winograd for valuable discussions, in particular about his results prior to publication.

[1] P. Sigmund, Phys. Rev. **184**, 383 (1969).
[2] R. Kelly, Phys. Rev. B **25**, 700 (1982).
[3] W.F. van der Weg and P.K. Rol, Nucl. Instrum. Methods **38**, 274 (1965).
[4] G.E. Thomas, Radiat. Eff. **31**, 185 (1977).
[5] M.L. Yu, in *Sputtering by Particle Bombardment III: Charged and Excited States of Sputtered Particles*, edited by R. Behrisch and K. Wittmaack (Springer-Verlag, Berlin, 1991).
[6] W.A. Metz, K.O. Legg, and E.W. Thomas, J. Appl. Phys. **51**, 2888 (1980).
[7] R.A. Baragiola, E.V. Alonso, and H.J.L. Raite, Phys. Rev. A **25**, 1969 (1982).
[8] N. Winograd, J. Phys. Chem. **96**, 6880 (1992).
[9] D.N. Bernardo, M. El-Maazawi, R. Maboudian, Z. Postawa, N. Winograd, and B.J. Garrison, J. Phys. Chem. **97**, 3846 (1992).
[10] H.D. Hagstrum, Phys. Rev. **96**, 336 (1954).
[11] G. Betz, Nucl. Instrum. Methods B **27**, 104 (1987).
[12] D. Grischkowsky, Ming L. Yu, and A.C. Balant, Surf. Sci. **127**, 331 (1983).
[13] W. Husinsky, G. Betz, and I. Girgis, Phys. Rev. Lett. **50**, 1689 (1983).
[14] W. Husinsky, J. Vac. Sci. Technol. B **5**, 1546 (1985).
[15] M.J. Pellin, R.B. Wright, and D.M. Gruen, J. Chem. Phys. **74**, 6448 (1981).
[16] M.J. Pellin, D.M. Gruen, C.E. Young, and M.D. Wiggins, Nucl. Instrum. Methods **218**, 771 (1983).
[17] E. Dullni, Appl. Phys. A **38**, 131 (1985).
[18] A. Wucher, W. Berthold, H. Oechsner, and K. Franzreb, Phys. Rev. A **49**, 2188 (1994).
[19] S.L. Chin and P. Lambropoulos, *Multiphoton Ionization of Atoms* (Academic, New York, 1984).
[20] S.R. Coon, W.F. Calaway, J.W. Burnett, M.J. Pellin, D.M. Gruen, D.R. Spiegel, and J.M. Spiegel, Surf. Sci. **259**, 275 (1991).
[21] A. Wucher, M. Wahl, and H. Oechsner, Nucl. Instrum. Methods B **82**, 337 (1993).
[22] W. Husinsky, G. Nicolussi, and G. Betz, Nucl. Instrum. Methods B **82**, 323 (1993).
[23] M.W. Thompson, Philos. Mag. **18**, 377 (1968).
[24] W. Hofer, in *Sputtering by Particle Bombardment III*, edited by R. Behrisch and K. Wittmaack (Springer-Verlag, Berlin, 1991).
[25] *Spectroscopic Data for Titanium, Chromium, and Nickel, Atomic Data for Fusion* Vol. VI, edited by W.L. Wiese and A. Musgrove (Controlled Fusion Atomic Data Center at Oak Ridge National Laboratory, Oak Ridge, 1989).
[26] E.B. Saloman, Spectrochim. Acta B **46**, 319 (1991).
[27] G. Nicolussi, W. Husinsky, and G. Betz, Phys. Rev. Lett. **71**, 1518 (1993).
[28] H. Oechsner and W. Gerhard, Surf. Sci. **44**, 480 (1974).
[29] H. Gnaser and W.O. Hofer, Appl. Phys. A **48**, 261 (1989).
[30] S.R. Coon, W.F. Calaway, M.J. Pellin, G.A. Curlee, and J.M. White, Nucl. Instrum. Methods B **82**, 329 (1993).
[31] C.E. Young, W.F. Calaway, M.J. Pellin, and D.M. Gruen, J. Vac. Sci. Technol. A **2**, 693 (1984).
[32] B. Schweer and H.L. Bay, in *Proceedings of the 4th International Conference on Solid Surface Science and 3rd European Conference on Surface Science*, edited by D.A. Degras and M. Costa (Societe Francaise du Vide, Paris, 1980), p. 1349.
[33] M.D. Morse, Chem. Rev. **86**, 1049 (1986).
[34] *Handbook of Chemistry and Physics*, 73rd ed., edited by D.R. Lide (CRC, Boca Raton, 1992).
[35] N. Andersen, B. Andresen, and E. Veje, Radiat. Eff. **60**, 119 (1982).
[36] P.J. Martin and R.J. MacDonald, Radiat. Eff. **32**, 177 (1977).
[37] W.F. van der Weg, N.H. Tolk, C.W. White, and J. Kraus, Nucl. Instrum. Methods **132**, 405 (1976).
[38] I.S.T. Tsong, N.H. Tolk, T.M. Buck, J.S. Kraus, T.R. Pian, and R. Kelly, Nucl. Instrum. Methods **194**, 655 (1982).
[39] G. Betz, R. Kirchner, W. Husinsky, F. Rüdenauer, and H.M. Urbassek, Radiat. Eff. Defects Solids **130-131**, 251 (1994).